Journal Name

ARTICLE TYPE

Cite this: DOI: 10.1039/xxxxxxxxxx

Supplementary information to the manuscript entitled "A new 2D monolayer BiXene, M_2C (M=Mo, Tc, Os)†"

Weiwei Sun[a*], **Yunguo Li**[b†], **Baotian Wang**[cd], **Xue Jiang**[e], **Mikhail I. Katsnelson**[fg], **Pavel Korzhavyi**[hi], **Olle Eriksson**[a], **Igor Di Marco**[a‡]

Received Date
Accepted Date

DOI: 10.1039/xxxxxxxxxx

www.rsc.org/journalname

In this Supplementary Information we first present our main results on the bulk parent materials of the 2D binary carbides discussed in the main manuscript. We have systematically investigated the structural properties of the possible binary carbides M_2C (M= Mo, Tc, Ru, Rh, Os). The energetically most favourable structures are shown to be strongly dependent on the number of valence electrons. The $P\bar{3}m1$ and $P63/mmc$ structures of Mo_2C and the $R3m$ and $P63/mmc$ structures of Tc_2C all show negative formation energies with respect to the elementary substances. This indicates that the corresponding bulk materials are highly likely to be synthesised. Moreover, calculated phonon dispersion relation curves for the two energetically most favourable structures of all M_2Cs are reported. These data show that the binary carbides have stable bulk structures from which the corresponding low dimensional materials (discussed in the main article) can be formed. In addition to the bulk materials, we also present results on some MAX phases that can be used to synthesise the monolayers. Finally, we have sections dedicated to the numerical errors in the phonon spectra and to the role of the spin-orbit coupling in the electronic structure calculations.

Bulk M_2Cs

In the main article we focus on the 2D material BiXene and its physical properties. The realisation of BiXene can be carried out from the bulk/thin films of these layered binary carbides. It is therefore important to present results obtained for the bulk M_2C (M=Mo, Tc, Ru, Rh, Os). We first study the thermodynamic and dynamic stability of the bulk M_2Cs in the $P\bar{3}m1$, $R3m$, $R\bar{3}m$, and $P63/mmc$ structures, illustrated in the panels (a)-(d) of Fig. 1 of the main manuscript.

These bulk structures have been either predicted by theoretical calculations[1,2] or reported by experiment[3] for Ru_2C and other 4d M_2C. We must mention that part of the data for Ru_2C have been already presented in our previous work[2]. There, we have also shown that the $R\bar{3}m$ phase is the most thermodynamically stable structure for Ru_2C, although we have to mention that another work, based on a less strict criterion for structural searching, predicted $P\bar{3}1m$ to be most favourable with respect to $R\bar{3}m$[4]. Essentially, the arrangement of M layers and C layers in $R3m$ and $R\bar{3}m$ follows the rules of growth which are common for MCs/MNs such as Re_2C[5] and Re_2N[6], and the $P\bar{3}1m$ phase has a higher energy per formula unit (f.u.). Concerning the other compounds, bulk Mo_2C exists in the Pbcn and $P\bar{3}m1$ structures[7], but can also be stabilised in the $P63/mmc$ structure on some substrates, like e.g. graphene[8]. Moreover, Juarez-Arellano *et al.*[5] predicted that at ambient conditions, in addition to Re_2C, also Os_2C should stabilise in the space group $P63/mmc$. They also found that Os_2C in the $P63/mmc$ structure is more stable than OsC in the WC or NiAs structures. These findings motivate us to exclude the *isotropic* hcp

[a]*Department of Physics and Astronomy, Materials theory, Uppsala University, Box 516, SE-75120 Uppsala, Sweden; *sun.weiwei@physics.uu.se; †*Corresponding author: Igor Di Marco, igor.dimarco@physics.uu.se*
[b]*Department of Earth Sciences, University College London, London WC1E 6BT, UK; †yunguo.li@ucl.ac.uk*
[c]*China Spallation Neutron Source (CSNS), Institute of High Energy Physics (IHEP), Chinese Academy of Sciences (CAS), Dongguan 523803, China*
[d]*Dongguan Institute of Neutron Science (DINS), Dongguan 523808, Chinaa*
[e]*Key Laboratory of Materials Modification by Laser, Ion and Electron Beams (Dalian University of Technology), Ministry of Education, Dalian 116024, China*
[f]*Radboud University of Nijmegen, Institute for Molecules and Materials, Heijendaalseweg 135, 6525 AJ Nijmegen, The Netherlands*
[g]*Theoretical Physics and Applied Mathematics Department, Ural Federal University, Mira Street 19, 620002 Ekaterinburg, Russia*
[h]*Department of Materials Science and Engineering, KTH-Royal Institute of Technology, Stockholm SE-10044, Sweden;*
[i]*Institute of Metal Physics, Ural Division of the Russian Academy of Sciences, 620219 Ekaterinburg, Russia*

† Electronic Supplementary Information (ESI) available: [details of any entary information available should be included here]. See DOI: 10.1039/b000000x/

Table 1 Calculated total energies (E_{tot}) and formation energies (E_{form}) per formula unit (f.u.) of the four investigated structures, for Os_2C, Rh_2C, Ru_2C, Tc_2C and Mo_2C. Note that data for Ru_2C have already been reported in our previous work[2] and are here presented only for an easier comparison.

	E_{tot} (eV/f.u.)			
Compound	$R3m$	$R\bar{3}m$	$P\bar{3}m1$	$P63/mmc$
Mo_2C	-30.737	-29.628	-31.307	-30.868
Tc_2C	-29.810	-29.343	-29.195	-30.099
Ru_2C	-26.640	-26.937	-26.183	-26.671
Rh_2C	-22.624	-22.848	-22.676	-22.579
Os_2C	-30.157	-30.877	-29.273	-30.139
	E_{form} (eV/f.u.)			
Compound	$R3m$	$R\bar{3}m$	$P\bar{3}m1$	$P63/mmc$
Mo_2C	0.228	1.337	-0.342	0.097
Tc_2C	-0.014	0.453	0.600	-0.303
Ru_2C	0.916	0.619	1.373	0.885
Rh_2C	0.987	0.763	0.935	1.032
Os_2C	1.399	0.679	2.283	0.914

structure (where the c/a ratio is close to one) from this work.

The total energies of the structures identified above for bulk M_2C (M=Mo, Tc, Ru, Rh, Os) are reported in Table 1, together with their formation energies (see Computational Details in the main text). The most likely stable structures showing negative formation energies are Mo_2C with $P\bar{3}m1$ symmetry, and Tc_2C with $R\bar{3}m$ and $P63/mmc$ symmetries. Moreover, the $P63/mmc$ structure of Mo_2C has a positive but very small formation energy, of 0.097 eV. For such a small value, the reference state used for calculating the formation energies may be important. For computational convenience (see main text), here we use the diamond structure of C, which is 0.03 eV/atom higher in energy than graphite, which is the ground-state[9]. We indeed calculated a more suitable value by including Van Der Waals interactions (see main text) and we obtained a formation energy of 0.05 eV, which is even smaller than in plain PBE. In general, energies of this scale are comparable to the entropy corrections K_BT, which ranges from 0.026 eV/atom at 298 K to 0.095 eV/atom at 1100 K[9]. Investigating these corrections in detail is beyond our scope but in any case our data suggest us to consider the $P63/mmc$ structure of Mo_2C as another possible stable structure. This is absolutely consistent with experimental results reporting the growth of thin films (up to 5 nm) of $P63/mmc$ Mo_2C on some substrates[8].

Apart from the structures mentioned in the previous paragraph, all other structures have positive formation energies. This does not necessarily mean that they cannot be produced, since the realisation of bulk metastable structures is indeed rather common for transition metal carbides and nitrides, and can be achieved by various techniques[10,11]. For example, Ru_2C has positive formation energies for both the $P\bar{3}m1$ and $R\bar{3}m$ structures but it can be realised in experiment via high pressure and high temperature synthesis[3]. It is not clear which one of these two structures is then measured at ambient conditions[2]. In any case, it is important to note that several structures in Table 1 are shown to have formation energies smaller than for the aforementioned Ru_2C (as well as other materials like e.g. PtN[12]). This suggests that although

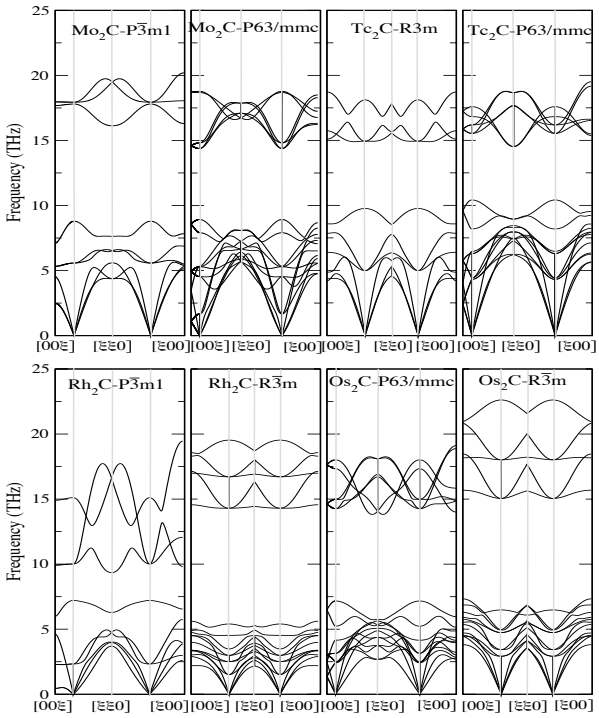

Fig. 1 Phonon dispersion curves of the first two favoured structures of M_2C (M=Mo, Tc, Rh, Os) bulk. Note that the phonon dispersion relation is expanded along the same path, so that the nodes may not be the high-symmetry points. This is aiming to make a straightforward comparison.

they are not possible to form at ambient conditions, they can probably be stabilised in thin films or other metastable structures. Here we focus on bulk Os_2C in the $P63/mmc$ structure, Rh_2C in the $P\bar{3}m1$ structure, and Tc_2C in the $P\bar{3}m1$, since they are related to the monolayers investigated in the main text. Given that their formation energies are of the same order as for the aforementioned Ru_2C, we can reasonably regard them as metastable structures. As mentioned above, to support this hypothesis, it was recently claimed that the Os_2C in the $P63/mmc$ structure is likely to form in a reaction in a carbon-saturated environment[13].

Although we investigate a limited number of compounds, an interesting trend may be inferred from the data in Table 1. Mo_2C has the smallest number of valence electrons in the 4*d* shell, and prefers to arrange in the $P\bar{3}m1$ structure. At half-filling, corresponding to Tc_2C, the most favourable structure becomes R3m. By adding more *d* electrons, e.g. for Ru_2C or Rh_2C, the $R\bar{3}m$ structure becomes the ground state. This is also the most favourable structure of Os_2C, which proves that the localization of the *d* electrons is not really a major factor for determining the structural stability. In the future we will extend these calculations to neighbouring elements and understand if this trend is confirmed or not.

For completeness, we also provide the optimised structural parameters of the investigated structures in Table 2. In $R3m$, one of the M atom occupies the $1a(\mu,\mu,\mu)$ Wyckoff position and another one the $1a(\nu,\nu,\nu)$ site; the C atom is located at the $1a(\omega,\omega,\omega)$ site. In $R\bar{3}m$, two of the M atoms occupy the $2c(\mu,\mu,\mu)$ Wyckoff positions and other two the $2c(\nu,\nu,\nu)$ sites; the two C atoms

Table 2 Optimized structural parameters of four phases for Mo_2C, Tc_2C, Ru_2C, Rh_2C, and Os_2C. Also the data of Ru_2C^a from Ref.[2] are reported, for an easier comparison.

Compound	Phase	Cell parameters	Coordinates
Mo_2C	$R3m$	a=5.498(Å), α=30.44°	μ=0.1366, ν=0.3143ω=0.8922
	$R\bar{3}m$	a=10.71 (Å), α=15.79°	μ= 0.6350, ν= 0.7710, ω=0.4784
	$P\bar{3}m1$	a=3.060 (Å), c=4.662 (Å)	z=0.2501
	$P63/mmc$	a=2.883 (Å), c=10.443 (Å)	z=0.1166
Tc_2C	$R3m$	a= 5.217(Å), α=31.48°	μ=0.1314, ν= 0.3173, ω=0.8945
	$R\bar{3}m$	a=10.79 (Å), α=14.83°	μ=0.6340, ν= 0.7705, ω=0.4783
	$P\bar{3}m1$	a=2.872 (Å), c=4.890 (Å)	z=0.2621
	$P63/mmc$	a=2.838 (Å), c=9.778 (Å)	z=0.1092
Ru_2C	$R3m^a$	a=5.293 (Å), α=30.35°	μ=0.1333, ν=0.3166, ω=0.8935
	$R\bar{3}m^a$	a=10.62 (Å), α=14.93°	μ=0.6328, ν=0.7704, ω=0.4777
	$P\bar{3}m1^a$	a=2.812 (Å), c=4.985 (Å)	z=0.2639
	$P63/mmc$	a=2.778 (Å), c=10.025 (Å)	z=0.1124
Rh_2C	$R3m$	a=5.358 (Å), α=30.23°	μ=0.1368, ν=0.3141, ω=0.8923
	$R\bar{3}m$	a=10.69 (Å), α=15.04°	μ=0.6334, ν= 0.7732, ω=0.4778
	$P\bar{3}m1$	a=2.974 (Å), c=4.689 (Å)	z=0.2458
	$P63/mmc$	a=2.794 (Å), c=10.241 (Å)	z=0.1172
Os_2C	$R3m$	a=5.352 (Å), α=30.32°	μ=0.1322, ν=0.3171, ω=0.8938
	$R\bar{3}m$	a=10.74 (Å), α=14.91°	μ=0.6322, ν=0.7703, ω=0.4777
	$P\bar{3}m1$	a=2.777 (Å), c=5.210 (Å)	z=0.2775
	$P63/mmc$	a=2.804 (Å), c=10.179 (Å)	z=0.1110

Table 3 The formation energy per formula unit of MAX, where M=Tc, Ru, Rh; A=Al, Si and X=C.

	Tc_2AlC	Tc_2SiC	Rh_2AlC	Rh_2SiC	Tc_2Ga_2C
E_{form} (eV)	-0.56	0.11	-0.36	0.47	+0.02

are located at the $2c(\omega,\omega,\omega)$ sites. In $P\bar{3}m1$, the two M atoms occupy the $2d(\frac{1}{3},\frac{2}{3},z)$ Wyckoff positions and the C atom locates at $1a$(0,0,0) site. In $P63/mmc$, the four M atoms occupy the $4f(\frac{1}{3},\frac{2}{3},z)$ Wyckoff positions and the two C atoms are located at the $2d(\frac{1}{3},\frac{2}{3},\frac{3}{4})$ site. Note that the primitive cells of the $R3m$ and $P\bar{3}m1$ phases contain only one formula unit, while the $R\bar{3}m$ structure consists of two formula units.

The phonon spectra of the energetically most and second most favoured structures (as identified from Table 1) are shown in Fig. 1. The data for Ru_2C are not shown since they can be found in Ref. 2. Fig. 1 illustrates clearly that the investigated structures are all dynamically stable. The dynamical stability and previously discussed formation energies identify which structures can be considered as stable. In our case we identify Mo_2C in the $P\bar{3}m1$ and $P63/mmc$ structures, as well as Tc_2C in the $R\bar{3}m$ and $P63/mmc$ structures as stable bulk systems. Moreover, on light of the discussion above, we suggest that Os_2C in the $P63/mmc$ structure, Rh_2C in the $P\bar{3}m1$ structure, and Tc_2C in the $P\bar{3}m1$ have good chances of being synthesised as metastable structures like e.g. as thin films.

Related MAX phases

It is known that 1T-monolayers (MXenes) were firstly synthesised via MAX phases[14]. In this work we suggest another possible way

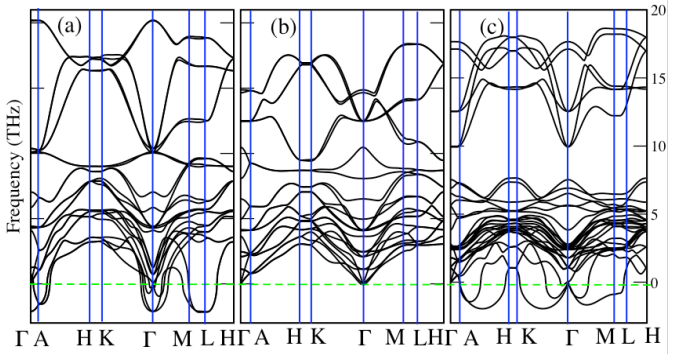

Fig. 2 The phonon dispersion curves of Tc_2AlC (a), Rh_2AlC (b) and Tc_2Ga_2C (c) along the path Γ-A-H-K-Γ-M-L-H.

of synthesis for 1T-M_2C monolayers via exfoliation from corresponding bulk materials. However, given that two of the three predicted 1T monolayers, i.e. 1T-Tc_2C and 1T-Rh_2C, are associated to bulk structures that cannot be directly synthesised at ambient conditions, it is also worth addressing the stability of a few related MAX phases. These may offer an alternative pathway to the experimental realisation of the predicted monolayers. In the following analysis we will not consider 1T-Mo_2C, since it not only has a corresponding stable bulk phase, i.e. Mo_2C in the $P\bar{3}m1$ structure, but has also already been synthesised from the MAX phase Mo_2Ga_2C[15,16]. In Table 3, we present formation energies of the MAX phases M_2XC, where M=Tc, Rh and X=Al, Si, as well as Tc_2Ga_2C. As we can see both Tc_2AlC and Rh_2AlC have negative formation energies. The calculated phonon spectra, which are reported in Fig. 2, show that Rh_2AlC has no imaginary mode, and

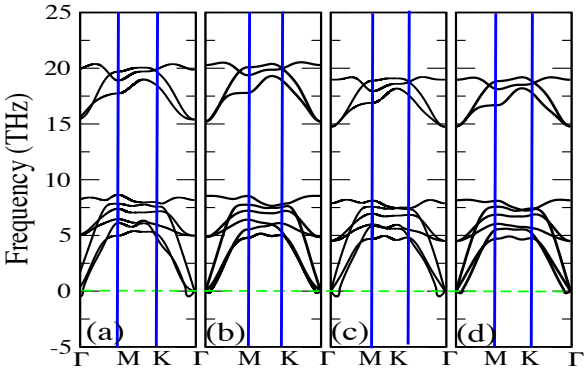

Fig. 3 The phonon dispersion curves of the free strain 1H-Mo_2C monolayer at zero temperature: (a) DFPT in LDA, using the structure optimized in LDA; (b) SDM in LDA, using the same structure optimized in LDA; (c) DFPT in PBE, using the structure optimized in PBE; (d) SDM in PBE, using the structure optimized in PBE.

is therefore likely to be synthesised. From it, we can expect to be able to create 1T-Rh_2C. Unfortunately, Tc_2AlC possesses rather large imaginary modes, which make it dynamically unstable. Inspired by the existence of Mo_2Ga_2C[15,16], the stability of the analogous MAX-phase Tc_2Ga_2C was explored, but we found a positive formation energy (Table 3) as well as a dynamically unstable phonon spectrum (Fig. 2, panel c).

Numerical errors in the phonon spectra

In this work we present phonon spectra calculated using the code PHONOPY in combination with VASP. Although this approach is based on the density functional perturbation theory (DFPT), a supercell is still needed, due to the lack of a transformation from the real space to the reciprocal space. Numerical truncation errors arise from the finite size of these supercells, and has to be added to the computational errors associated to other minor technical details.

To have an idea of the errors associated to the numerical truncation, we also calculated selected phonon spectra through the small displacement method (SDM), as implemented in the Phon code[17]. A comparison between the phonon spectra obtained with DFPT (PHONOPY+VASP) and those obtained with SDM (Phon+VASP) is reported in Fig. 3, for both LDA and PBE. This picture shows that the imaginary modes are still present in the SDM spectra, but strongly quenched with respect to the calculations performed via DFPT. The temperature induced stabilization, which is discussed in the main text, is even easier in this case.

Effects of spin-orbit coupling

It is important to have an idea to what extent the spin-orbit coupling is going to affect the physical properties of our systems. The formation energies of the monolayers, reported in Table 1 of the main manuscript, are all between 0.5 and 1 eV per atom. Including spin-orbit coupling is not going to change this scenario since the energy corrections to these values are expected to be at least one order of magnitude smaller. The phonon spectra of materials involving 4*d* and 5*d* elements can in principle undergo

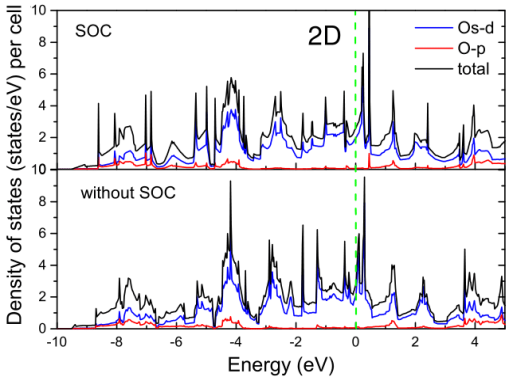

Fig. 4 The projected DOS of 1H-Os_2C, with and without spin-orbit coupling (SOC), in the upper and lower panels respectively. In these plots, the blue curves stand for Os-d states, the red curves for O-p states, and the black curves for the total DOS.

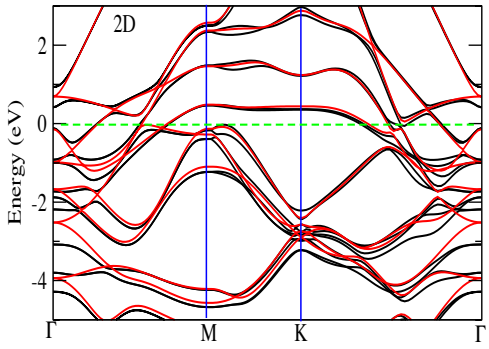

Fig. 5 The band structure of 1H-Os_2C, with and without spin-orbit coupling (SOC), corresponding to black and red curves respectively.

bigger changes, but those are related to the changes induced in the electronic bonding. These can in turn be analysed by looking at the electronic structure directly. Among the studied materials, Os_2C contains Os, which is the heaviest element addressed in this work. Therefore we will consider 1H-Os_2C as an illustrative example. We calculated the electronic structure of 1H-Os_2C to analyse to what extent the electronic properties are modified by the spin-orbit coupling. The computational details are analogous to those described in the section "Computational details" of the main manuscript. In Fig. 4 we report a comparison of the projected density of states (DOS), with and without spin-orbit coupling. The two plots show a very similar distribution of spectral weight. The only noticeable differences are the splitting of some peaks. A more detailed analysis can be obtained by looking at the corresponding band structure, reported in Fig. 5. The changes induced by the spin-orbit coupling are visible, but do not seem to change the character of the bands crossing the Fermi energy. From this band structure, it is also clear that the Fermi surface, and in turn all related properties, are not much affected by the presence of spin-orbit coupling. This physical picture corresponds to small changes in the phonon spectra as well, and is analogous to what found in other studies, like e.g. in a recent work involving Pt compounds [18]. Finally, the remaining carbides are composed of elements that are much lighter than Os, and therefore the effects due to spin-orbit coupling are expected to be much smaller than for Os_2C.

References

1 E. Deligoz, H. B. Ozisik, K. Colakoglu and Y. O. Ciftci, *Mater. Sci. Tech.*, 2014, **30**, 842.

2 W. Sun, Y. Li, L. Zhu, Y. Ma, I. Di Marco, B. Johansson and P. Korzhavyi, *Phys. Chem. Chem. Phys.*, 2015, **17**, 9730.

3 N. R. S. Kumar, N. V. C. Shekar, S. Chandra, J. Basu, R. Divakar and P. C. Sahu, *J. Phys.: Condens. Matter.*, 2012, **24**, 362202.

4 F. H. Jian Lu, W. Lin, W. Ren, Y. Li and Y. Yan, *J. Phys.: Condens. Matter.*, 2015, **27**, 175505.

5 E. A. Juarez-Arellano, B. Winkler, A. Friedrich, L. Bayarjargal, V. Milman, J. Yan and S. M. Clark, *J. Alloys and Compds.*, 2009, **481**, 577.

6 A. Friedrich, B. Winkler, L. Bayarjargal, W. Morgenroth and E. A. Juarez-Arellano, *Phys. Rev. Lett.*, 2010, **105**, 085504.

7 E. Parthé and V. Sadagopan, *Acta Cryst.*, 1963, **16**, 202–205.

8 C. He and J. Tao, *Chem. Commun.*, 2015, **16**, 8323–8325.

9 D. R. Kania, *The Physics of Diamond, Proceedings of the International School of Physics "Enrico Fermi", in Course CXXXV*, IOS Press, Amsterdam; SIF, Bologna, 1997.

10 E. Gregoryanz, C. Sanloup, M. Somayazulu, J. Badro, G. Fiquet, H. Mao and R. J. Hemley, *Nat. Mater.*, 2004, **3**, 294.

11 S. T. Oyama, *The Chemistry of Transition Metal Carbides and Nitrides*, Springer Netherlands, Dordrecht, 1996.

12 M. S. H. Suleiman and D. P. Joubert, arXiv:1301.5490.

13 E. A. Juarez-Arellano, B. Winkler, A. Friedrich, L. Bayarjargal, V. Milman, J. Yan and S. M. Clark, *Journal of Alloys and Compounds*, 2009, **481**, 577–581.

14 M. Naguib, O. Mashtalir, J. Carle, V. Presser, J. Lu, L. Hultman, Y. Gogotsi and M. W. Barsoum, *ACS Nano*, 2012, **6 (2)**, 1322–1331.

15 J. Halim, S. Kota, M. R. Lukatskaya, M. Naguib, M.-Q. Zhao, E. J. Moon, J. Pitock, J. Nanda, S. J. May, Y. Gogotsi and M. W. Barsoum, *Adv. Funct. Mater.*, 2016, **26**, 3118–3127.

16 R. Meshkian, L.-A. Näslund, J. Halim, J. Lu, M. W. Barsoum and J. Rosen, *Scripta Materialia*, 2015, **108**, 147–150.

17 D. Alfé, *Computer Physics Communications*, 2009, **180**, 2622–2633.

18 X.-Q. Zhang, Z.-Y. Zeng, Y. Cheng and G.-F. Ji, *RSC Adv.*, 2016, **6**, 27060–27067.